

**TRIBOPOLYMERIZATION: ANTI-WEAR BEHAVIOR OF NEW  
HIGH-TEMPERATURE ADDITIVE CLASSES**

By:

**Jeffrey Joseph Valentino**

Thesis Submitted to the Faculty of  
Virginia Polytechnic Institute and State University  
in Partial Fulfillment of the Requirements for the Degree of

**Master of Science**

**In**

**Mechanical Engineering**

Michael J. Furey, Ph.D., Chairman

Norman S. Eiss, Jr., Ph.D.

Brian Vick, Ph.D.

February, 2000  
Blacksburg, Virginia

Keywords: Tribology, Ceramics, Lubrication, Tribopolymerization, Anti-wear, Alumina

Copyright 2000, Jeffrey J. Valentino

# **Tribopolymerization: Anti-wear Behavior of New High-Temperature Additive Classes.**

Jeffrey Joseph Valentino

## **ABSTRACT**

Advanced ceramic materials have found many new applications in the automotive and other industries. To satisfy demands of higher temperatures and inert surfaces, new lubrication methods for these ceramics need explored and evaluated. This thesis focuses on a boundary lubrication method termed tribopolymerization -- the formation of polymers at the tribological interphase. The research evaluated new high-temperature classes of anti-wear additives. The work involved experiments on steel and alumina material pairs with a pin-on-disk tribometer used to explore the anti-wear capabilities of selected additives in the liquid phase at concentrations of 1% by weight in hexadecane.

New additives included aromatic compounds with various pendant groups adding the design functionality necessary for in-situ polymerization. The amino, hydroxyl, acid, and ester functional groups underwent studies across several aromatic molecular compositions while new heterocyclic additives, in particular the readily available lactams, underwent exploratory tests as a new class under the tribopolymerization design approach. In concentrations of 1%, additives showed significant wear reductions of up to 99.9 %. Anti-wear behavior persisted in select cases at concentrations as low as 0.1% by weight. Compounds from two new classes demonstrated anti-wear behavior at 6x the frictional heat generation of standard exploratory conditions. This surprising effect partially filled a void in the effective range of operating conditions between 0.25 m/s, 40 N and 1.0 m/s, 160 N. Earlier work by Tritt found a complete absence of anti-wear behavior for the previous additive classes at the high-speed conditions.

In addition, several individual compounds constituent to an A-R-A + B-R'-B condensation polymerization reaction demonstrated significant anti-wear behavior when used alone. In particular, the compound BTDA from DuPont's Kapton ® exhibited higher wear reductions than any other new additive.

These findings support tribopolymerization as an effective approach to boundary lubricant design. Low wear was often associated with an attached reaction debris layer. This finding is consistent with previous work involving tribopolymerization anti-wear additives with ceramics. Further research into the roles of the debris layer and tribochemistry will help in understanding the complex anti-wear behavior of these new high-temperature additive classes.

## ACKNOWLEDGMENTS

The completion of this research and thesis was due in large part to the generous contributions of friends, family, faculty, staff and the United States Department of Energy (DOE). Dr. Michael J. Furey contributed foremost in the sum of his efforts to mentor, educate and advise me in the field of study and I thank him for his service as Committee Chairman. A sincere thanks goes to the venerable Dr. Norman S. Eiss for dependable advice, perspective and assistance with metrology equipment, and to Dr. Brian Vick for serving as committee members. Dr. Czeslaw Kajdas, Dr. Roman Kempinski, and Dr. Bhawani Tripathy, thank you for your selfless contributions in time, energy and support. I thank Mr. Frank Kromer for his experience and operation of the XPS equipment in Virginia Tech Chemistry Department's Surface Analysis Lab.

I am grateful for the financial support afforded by the DOE Energy Related Invention Program, its administrators and the taxpayers. Without their recognition of Dr. Furey's proposal as a promising energy-related invention, none of this research would have been possible. I thank all those researchers who paved the way to this point, many of whom are referenced throughout the text. In particular I recognize Chris Smith for his development of the pin-on-disk device, Ben Tritt for modifications and work leading up to this phase, and Dr. Bhawani Tripathy for his excellent pioneering research and dissertation.

A deep gratitude is felt to patient and supportive family members, namely my mother and father, Anne and Ralph Valentino, brothers Gregory and Matthew, and loving sister Jennifer and family. Also, I would like to recognize Jon Fritsch and Eric Yount for their continuing motivation and friendship in all aspects of my graduate experience. A special thanks goes to fellow researcher Michael Owellen for two years of collaboration in research and life. I thank Srikrishna Talluri for his support, insight and friendship. I also would like to acknowledge the researchers and friends LaShaun Berrien, Anne-Claire Christiaen, and Gustavo Molina for their cooperation and comradery.

## TABLE OF CONTENTS

ABSTRACT.....	ii
ACKNOWLEDGMENTS .....	iii
TABLE OF CONTENTS .....	iv
LIST OF FIGURES .....	vi
LIST OF TABLES .....	xiii
1. INTRODUCTION .....	1
1.1 Rationale .....	1
1.2 Objectives.....	2
2. LITERATURE REVIEW .....	4
2.1 Lubricant Development.....	4
2.2 Ceramic Applications.....	5
2.3 Conventional Ceramic Lubrication.....	8
2.4 Recent Developments in Ceramic Lubrication.....	9
2.5 Ceramic Wear Mechanisms.....	11
2.6 Tribopolymerization .....	13
2.7 High-temperature monomer additives .....	17
3. EXPERIMENTAL .....	20
3.1 Introduction.....	20
3.2 Pin-on-Disk Device.....	20
3.3 Tribological Materials.....	21
3.4 Lubricants .....	22
3.5 Procedure.....	24
3.6 Sample Analysis.....	25
4. RESULTS.....	27
4.1 Steel-on-Steel Tests.....	27
4.1.1 Hexadecane Reference.....	28
4.1.2 A-R-B Tribomonomers.....	30
4.1.3 A-R-A + B-R'-B Type Compounds .....	36
4.1.4 Caprolactam .....	38

4.2 Alumina A System.....	40
4.2.1 Hexadecane Reference.....	40
4.2.2 A-R-B Type Tribonomers.....	45
4.2.3 A-R-A + B-R'-B Type Compounds.....	55
4.2.4 Caprolactam.....	62
4.3 Alumina B System.....	68
4.3.1 Hexadecane Reference.....	68
4.3.2 A-R-B Type Tribonomers.....	74
4.3.3 A-R-A + B-R'-B Type Compounds.....	77
4.3.4 Cyclic amides.....	86
4.3.5 A-R-A or B-R'-B Type Compounds Alone.....	88
4.3.6 Other Compounds.....	91
5. DISCUSSION.....	94
5.1 Objectives.....	94
5.2 Steel System.....	94
5.3 Alumina A System.....	96
5.4 Alumina B System.....	98
5.5 Parametric Studies.....	101
6. CONCLUSIONS.....	108
7. RECOMMENDATIONS.....	110
REFERENCES.....	111
APPENDICES.....	115
Appendix A: Wear Data.....	115
Vita.....	121

## List of Figures

<b>Figure 2.5.1</b>	Effect of Load on Relative Wear for Several Tribomonomers .....	16
<b>Figure 3.4.1</b>	New Tribopolymerization Molecular Classes and Structures.....	23
<b>Figure 4.1.1.1</b>	Hexadecane Reference Tests in Order by Total Wear, Steel System.....	28
<b>Figure 4.1.1.2</b>	Ball Percentage of Total Wear Volume for Hexadecane Reference Tests in Steel System .....	29
<b>Figure 4.1.1.3</b>	Photomacrographs of Disk Wear Tracks for Hexadecane Reference Tests at 40 x (All rinsed except Test 23) .....	30
<b>Figure 4.1.2.1</b>	Anti-wear Effects of Aromatic Hydroxy Acids in Steel System.....	31
<b>Figure 4.1.2.2</b>	Photomacrographs of 4-Hydroxy Benzoic Acid Disk Wear Track in Steel System (after methanol rinse).....	32
<b>Figure 4.1.2.3</b>	Photomacrographs of 4-Hydroxy Cinnamic Acid Disk Wear Track in Steel System (after methanol rinse).....	32
<b>Figure 4.1.2.4</b>	Anti-wear Effects of Aromatic Amino Acids in Steel System.....	33
<b>Figure 4.1.2.5</b>	Photomacrographs of 4-Amino Benzoic Acid Disk Wear Track in Steel System .....	33
<b>Figure 4.1.2.6</b>	Photomacrographs of 4-Amino Phenylacetic Acid Disk Wear Track in Steel System .....	34
<b>Figure 4.1.2.7</b>	Anti-wear Effect of Aromatic Amino Ester in Steel System .....	35
<b>Figure 4.1.2.8</b>	Photomacrographs of Ethyl-4-Amino Benzoate Disk Wear Track in Steel System .....	35
<b>Figure 4.1.3.1</b>	Anti-wear Effect of A-R-A + B-R'-B Compounds Dimethyl Terephthalate and Tert-Butyl Hydroquinone in Steel System.....	36
<b>Figure 4.1.3.2</b>	Photomacrographs of Equimolar Mixture of Compounds Dimethyl Terephthalate and Tert-Butyl Hydroquinone Disk Wear Track in Steel System .....	37
<b>Figure 4.1.4.1</b>	Anti-wear Effect for the Heterocyclic Amide Caprolactam .....	38

<b>Figure 4.1.4.2</b>	Photomacrographs of Caprolactam Disk Wear Track in Steel System.....	39
<b>Figure 4.2.1.1</b>	Alumina A System Hexadecane Reference Tests .....	41
<b>Figure 4.2.1.2</b>	Alumina A System Reference, Test 26: Photomacrograph of Disk Wear Track (15.75 x).....	42
<b>Figure 4.2.1.3</b>	Alumina A System Reference, Test 27: Photomacrograph of Disk Wear Track (15.75 x).....	43
<b>Figure 4.2.1.4</b>	Alumina A System Reference, Test 28: Photomacrograph of Disk Wear Track (15.75 x).....	43
<b>Figure 4.2.1.5</b>	Alumina A System Reference, Test 29: Photomacrograph of Disk Wear Track (15.75 x).....	44
<b>Figure 4.2.1.6</b>	Alumina A System Reference, Test 40: Photomacrograph of Disk Wear Track (15.75 x).....	44
<b>Figure 4.2.1.7</b>	Alumina A System Reference, Test 41: Photomacrograph of Disk Wear Track (15.75 x).....	45
<b>Figure 4.2.2.1</b>	Anti-wear Effect of Aromatic Amino Acid in Alumina A System .....	46
<b>Figure 4.2.2.2</b>	Anti-wear Effect of Aromatic Amino Ester in Alumina A System .....	47
<b>Figure 4.2.2.3</b>	Ethyl-4-Amino Benzoate in Alumina A System, Test 32: Photomacrograph of Disk Wear Track (15.75 x).....	47
<b>Figure 4.2.2.4</b>	Ethyl-4-Amino Benzoate in Alumina A System, Test 32: Photomacrograph of Ball Wear Area (15.75 x).....	48
<b>Figure 4.2.2.5</b>	Ethyl-4-Amino Benzoate in Alumina A System, Test 33: Photomacrograph of Disk Wear Track (15.75 x).....	48
<b>Figure 4.2.2.6</b>	Filtered Ethyl-4-Amino Benzoate in Alumina A System, Test 42: Photomacrograph of Disk Wear Track (15.75 x).....	49
<b>Figure 4.2.2.7</b>	Filtered Ethyl-4-Amino Benzoate in Alumina A System, Test 42: Photomacrograph of Ball Wear Area (15.75 x).....	50
<b>Figure 4.2.2.8</b>	Filtered Ethyl-4-Amino Benzoate in Alumina A System, Test 42: Photomacrograph of Ball Wear Area (40 x) .....	50

<b>Figure 4.2.2.9</b> Filtered Ethyl-4-Amino Benzoate in Alumina A System, Test 42: Photomacrograph of Ball Wear Area (80 x) .....	51
<b>Figure 4.2.2.10</b> Anti-wear Effect of Aromatic Hydroxy Ester in Alumina A System .....	52
<b>Figure 4.2.2.11</b> Methyl-4-Hydroxy Benzoate in Alumina A System, Test 34: Photomacrograph of Disk Wear Track (15.75 x) .....	53
<b>Figure 4.2.2.12</b> Methyl-4-Hydroxy Benzoate in Alumina A System, Test 34: Photomacrograph of Ball Wear Area (15.75 x) .....	53
<b>Figure 4.2.2.13</b> Methyl-4-Hydroxy Benzoate in Alumina A System, Test 34: Photomacrograph of Ball Wear Area (15.75 x) .....	54
<b>Figure 4.2.2.14</b> Methyl-4-Hydroxy Benzoate in Alumina A System, Test 34: Photomacrograph of Ball Wear Area (15.75 x) .....	54
<b>Figure 4.2.3.1</b> Anti-wear Effect of A-R-A + B-R'-B Compounds Dimethyl Terephthalate and Tert-Butyl Hydroquinone in Alumina A System .....	55
<b>Figure 4.2.3.2</b> Dimethyl Terephthalate and Tert-Butyl Hydroquinone in Alumina A System, Test 38: Photomacrograph of Disk Wear Track (15.75 x).....	56
<b>Figure 4.2.3.3</b> Dimethyl Terephthalate and Tert-Butyl Hydroquinone in Alumina A System, Test 38: Photomacrograph of Disk Wear Track (15.75 x).....	57
<b>Figure 4.2.3.4</b> Dimethyl Terephthalate and Tert-Butyl Hydroquinone in Alumina A System, Test 38: Photomacrograph of Disk Wear Track (40 x) .....	57
<b>Figure 4.2.3.5</b> Dimethyl Terephthalate and Tert-Butyl Hydroquinone in Alumina A System, Test 38: Photomacrograph of Ball Wear Area (40 x) .....	58
<b>Figure 4.2.3.6</b> Dimethyl Terephthalate and Tert-Butyl Hydroquinone in Alumina A System, Test 38: Photomacrograph of Ball Wear Area (80 x) .....	58
<b>Figure 4.2.3.7</b> Dimethyl Terephthalate and Tert-Butyl Hydroquinone in Alumina A System, Test 38: Photomacrograph of Ball Wear Area (80 x) .....	59
<b>Figure 4.2.3.8</b> Dimethyl Terephthalate and Tert-Butyl Hydroquinone in Alumina A System, Test 39: Photomacrograph of Ball Wear Area (80 x) .....	59

<b>Figure 4.2.3.9</b> Filtered Dimethyl Terephthalate and Tert-Butyl Hydroquinone in Alumina A System, Test 44: Photomacrograph of Disk Wear Track (15.75 x).....	60
<b>Figure 4.2.3.10</b> Filtered Dimethyl Terephthalate and Tert-Butyl Hydroquinone in Alumina A System, Test 44: Photomacrograph of Disk Wear Track (40 x).....	61
<b>Figure 4.2.3.11</b> Filtered Dimethyl Terephthalate and Tert-Butyl Hydroquinone in Alumina A System, Test 44: Photomacrograph of Ball Wear Area (40 x).....	61
<b>Figure 4.2.4.1</b> Anti-wear Effect of Caprolactam in Alumina A System .....	62
<b>Figure 4.2.4.2</b> Caprolactam in Alumina A System, Test 30: Photomacrograph of Disk Wear Track (40 x) .....	63
<b>Figure 4.2.4.3</b> Caprolactam in Alumina A System, Test 31: Photomacrograph of Disk Wear Track (40 x) .....	63
<b>Figure 4.2.4.4</b> Caprolactam in Alumina A System, Test 30: Photomacrograph of Ball Wear Area (80 x).....	65
<b>Figure 4.2.4.5</b> Caprolactam in Alumina A System, Test 31: Photomacrograph of Ball Wear Area (80 x).....	65
<b>Figure 4.2.4.6</b> Filtered Caprolactam in Alumina A System, Test 43: Photomacrographs of Wear Areas.....	66
<b>Figure 4.2.4.7</b> Filtered Caprolactam in Alumina A System, Test 43: Photomacrograph of Ball Wear Area (40 x) .....	66
<b>Figure 4.2.4.8</b> Filtered Caprolactam in Alumina A System, Test 43: Photomacrograph of Ball Wear Area, External Lighting (80 x).....	67
<b>Figure 4.2.4.9</b> Filtered Caprolactam in Alumina A System, Test 43: Photomacrograph of Ball Wear Area, Internal Lighting (80 x).....	67
<b>Figure 4.3.1.1</b> Hexadecane Reference Wear Volumes in Ascending Order for Alumina B System .....	70
<b>Figure 4.3.1.2</b> Disk Photomacrographs from Hexadecane Reference Tests.....	71
<b>Figure 4.3.1.3</b> Ball Photomacrographs from Hexadecane Reference, Test 90 .....	72

<b>Figure 4.3.1.4</b>	Ball Photomicrographs from Hexadecane Reference, Test 131 .....	73
<b>Figure 4.3.1.5</b>	Ball Photomicrographs from Hexadecane Reference, Test 137 .....	73
<b>Figure 4.3.2.1</b>	Anti-wear Effect of Aliphatic Amino Acid in Alumina B System.....	74
<b>Figure 4.3.2.2</b>	Photomicrographs of 6-Aminocaproic Acid Wear Areas, Test 107 (a) ball, 40x, int. + ext. lighting, after hexane rinse (b) disk, 40x, int. + ext. lighting.....	75
<b>Figure 4.3.2.3</b>	Photomicrographs of 6-Aminocaproic Acid Wear Areas, Test 108 (a) ball, 40x, int. + ext. lighting, (b) disk, 40x, int. + ext. lighting.....	75
<b>Figure 4.3.2.4</b>	Anti-wear Effect of Aromatic Amino Ester in Alumina B System .....	76
<b>Figure 4.3.2.5</b>	Photomicrographs of Ethyl-4-Aminobenzoate Wear Areas after methanol rinse, (a) Test 158 ball, 15.75x, int. + ext. lighting, (b) Test 51 disk, 15.75x, int. + ext. lighting. ....	76
<b>Figure 4.3.3.1</b>	Anti-wear Effects of A-R-A + B-R'-B Compounds Tert-butyl Hydroquinone and Isomers of Dimethyl Phthalate in Alumina B System.....	77
<b>Figure 4.3.3.2</b>	Anti-wear Effect of A-R-A + B-R'-B Compounds ODA and BTDA in Alumina B System. ....	78
<b>Figure 4.3.3.3</b>	Photomicrographs of ODA+BTDA Ball Wear Areas after methanol rinse, (a) Test 109, 40x, int. + ext. lighting (b) Test 109, 40x, int. + ext. lighting, (c) Test 109, 80x int. lighting, (d) Test 109, 80x int. + ext. lighting, (e) Test 115, 80x, ext. lighting, (f) Test 115, 80x, int. lighting. ....	80
<b>Figure 4.3.3.4</b>	Photomicrographs of ODA+BTDA Disk Wear Tracks after methanol rinse, Test 115 disk (a) 15.75x, ext. lighting, (b) 40x, ext. lighting, (c) 80x, ext. lighting, (d) 40x, int. lighting.....	81
<b>Figure 4.3.3.5</b>	Photomicrographs of ODA + BTDA Disk Wear Tracks, Test 109 (a) 40x, ext. lighting, (b) 40x, int. lighting., (c) 80x, ext. lighting, (d) 80x, int. lighting. ....	81
<b>Figure 4.3.3.6</b>	Anti-wear Effect of A-R-A + B-R'-B Compounds ODA and BTDA in Alumina B System 2x2 Load/Speed Matrix.....	82

<b>Figure 4.3.3.7</b>	Photomicrographs of ODA + BTDA 2x2 Matrix Ball Wear Areas, (a) Test 115, 40x, ext. lighting, (b) Test 119, 40x, ext. lighting, (c) 40x, ext. lighting, (d) 40x, ext. lighting .....	84
<b>Figure 4.3.3.8</b>	Photomicrographs of ODA + BTDA 2x2 Matrix Disk Wear Tracks, (a) Test 115, 15.75x, ext. lighting, (b) Test 125, 15.75x, ext. lighting, (c) 15.75x, ext. lighting, (d) 15.75x, ext. lighting.....	84
<b>Figure 4.3.3.9</b>	Photomicrographs of ODA + BTDA 2x2 Matrix Disk Wear Tracks, (a) Test 115, 40x, int. lighting, (b) Test 125, 40x, ext. lighting, (c) Test 128, 40x, ext. lighting, (d) Test 123, 40x, ext. lighting .....	85
<b>Figure 4.3.3.10</b>	Photomicrographs of ODA + BTDA 2x2 Matrix Ball Wear Areas, (a) Test 115, 80x, int. lighting, (b) Test 125, 40x, ext. lighting, (c) Test 128, 40x, ext. lighting, (d) Test 123, 40x, ext. lighting, (e) Test 128, 80x, ext. lighting, after hexane rinse, (f) Test 123, 80x, ext. lighting after hexane rinse .....	86
<b>Figure 4.3.4.1</b>	Anti-wear Effect of Cyclic Amide Class in Alumina B System .....	87
<b>Figure 4.3.4.2</b>	Anti-wear Effect of Caprolactam in Alumina B System 2x2 Load/Speed Matrix .....	88
<b>Figure 4.3.5.1</b>	Anti-wear Effects of A-R-A or B-R'-B Compounds Tert-Butyl Hydroquinone and Dimethyl Phthalate Isomers Alone in Alumina B System .....	89
<b>Figure 4.3.5.2</b>	Photomicrographs of Tert-Butyl Hydroquinone Ball Wear, (a) Test 159, 15.75x, int/ext. lighting, (b) Test 159, 40x, int/ext. lighting .....	89
<b>Figure 4.3.5.3</b>	Anti-wear Effects of A-R-A + B-R'-B Compounds Alone in Alumina B System .....	90
<b>Figure 4.3.5.4</b>	Photomicrographs of ODA Alone, Ball Wear Area, Test 151, (a) 15.75x, int./ext. lighting, after methanol rinse (b) 40x, int./ext. lighting, after methanol rinse. ....	91
<b>Figure 4.3.5.5</b>	Photomicrographs of BTDA Alone Wear Areas, Test 153, (a) 15.75x, int./ext. lighting., after methanol rinse (b) 40x, int./ext. lighting, after methanol rinse, (c) 7.9x, ext. lighting, (d) 15.75x, ext. lighting.....	91
<b>Figure 4.3.6.1</b>	Anti-wear Effects of Other Compounds in Alumina B System .....	92

**Figure 4.3.6.2** Photomacrographs of Monoester Wear Areas, Test 171, (a) 40x, ext. lighting., after methanol rinse (b) 80x, int./ext. lighting, after methanol rinse, (c) 15.75x, int. lighting, (d) 40x, ext. lighting. ....93

**Figure 5.1** Effect of Load on Relative Wear for Several Tribomonomers..... 104

## LIST OF TABLES

Table 2.1	Ceramics in Tribology .....	6
Table 3.1	Test Specimens .....	21
Table 5.1	Steel System Summary .....	96
Table 5.2	Alumina A System Summary .....	98
Table 5.3	Alumina B System Summary .....	100
Table 5.4	High Speed High Load Results: Tritt's Study .....	105
Table 5.5	High Speed High Load Results: Current Study .....	105
Table A1	Wear Data for Steel System .....	115
Table A2	Wear Data for Alumina A System .....	116
Table A3	Wear Data for Alumina B System.....	117

## Chapter 1

# INTRODUCTION

### 1.1 Rationale

Friction, wear and lubrication are studied in the field of tribology. Research in this field aims to enable, improve or economize existing and new material and engineering technologies. Materials science has developed ceramics into a promising new solution to some structural and tribological material selection problems. As a structural material, ceramics offer high hardness, high thermal stability, low density and low thermal conductivity. Using ceramics in tribological systems takes advantage of these properties as well as the advantageous tribological properties of excellent wear resistance and chemical stability. Ceramics have entered a wide range of demanding, yet practical applications such as cutting tools and high-speed bearings. The adiabatic internal combustion engine is an example of a severe tribological system for which suitable ceramics and lubricants require research and development. Ceramics present enabling material properties for new applications and economical, durable replacements for existing applications.

Ceramics however, have presented challenges to the lubrication engineer, particularly in the boundary lubrication regime where direct contact occurs. Their unreactive surfaces tend to disable anti-wear and extreme pressure additives' surface interactions while the desired maximum operating temperatures approach and exceed the limits of liquid organic lubricant carriers and additives.

Tribopolymerization is the in-situ polymerization initiated and propagated by the mechanical, chemical and thermal environment present at or near a rubbing surface. This

lubrication approach can function in the presence of any one or combination of appropriate environments and its potential is therefore independent of substrate. Lubrication by tribopolymerization has been successfully applied to both metal and ceramic material interfaces. This study focuses on tribopolymerization as an approach to ceramic lubrication as part of the United State's Department of Energy's Energy-Related-Invention Program (DOE/ERIP). More specifically, this research explores new classes of ashless organic compounds as anti-wear additives, herein termed "tribomonomers," which are capable of tribopolymerization. Energy savings are sought by finding effective wear-reducing tribomonomers with chemical structures or compositions that lead to tribopolymers which either form at higher temperatures and/or withstand higher temperatures.

## **1.2 Objectives**

Previous research efforts have focused on two broad areas: (1) the effects of various operating conditions such as load, speed, and temperature on anti-wear behavior in the boundary regime, and (2) identification and characterization of surface films. The core of the research focused on a select six -- proven tribomonomers in liquid and vapor phase pin-on-disk testing. This study is an exploratory investigation into liquid based anti-wear action of several new classes of tribomonomers chosen based on molecular structural and functional attributes that typically provide improved thermal stability. Various classes of additive compounds were tested under one or more material systems and operating conditions to explore the potential of these new tribopolymerization classes as boundary lubricants.

Specifically, the major objectives of this study are:

- 1) To continue to use the tribopolymerization model as an anti-wear approach for ceramics.
- 2) To explore the anti-wear capabilities of tribomonomers with amino and aromatic content.
- 3) To evaluate promising anti-wear behavior and/or economical additives at higher loads and speeds.
- 4) To identify and characterize any tribochemical changes evident in surface films formed from the boundary energy environment.

## Chapter 2

### **LITERATURE REVIEW**

The central theme of this research is tribopolymerization as a novel approach to ceramic lubrication. Thusly, a review of literature and patents pertaining to lubrication, ceramics, and tribopolymerization is presented next. A short background discussion of lubricant development is presented in Section 2.1, followed by an introduction to ceramic tribological properties and applications in Section 2.2. Shortcomings of conventional ceramic lubrication are highlighted in Section 2.3, illustrating the need for the novel approach of tribopolymerization. Several recently developed methods of high temperature and/or ceramic lubrication are reviewed in Section 2.4 followed by a survey of ceramic wear mechanisms in Section 2.5. Next in Section 2.6, major milestones in the ongoing exploration into tribopolymerization are discussed followed by significant results, conclusions and recommendations leading up to this investigation into high temperature additives (particularly for ceramics). Finally, polymer chemistry principles related to thermal stability and structure relationships are discussed.

#### **2.1 Lubricant Development**

The evolution of the modern lubricating oils and greases can be traced back to the discovery of techniques for producing petroleum from coal. Increased availability of crude oil due to drilling discoveries in Titusville, Pennsylvania by Drake gave birth to a large market for many petroleum-based products including gasoline and lubricating oils. These two products grew together in demand with the advent of the internal combustion engine and its application to personal automobiles. Increased demand on lubricant durability increased slowly in proportion to industrial and market factors until the

impetus provided by World War II. The need for better performance in existing lubricant applications and the development of new lubricants (synthetics) for the more demanding machinery and environments of the war effort attracted the research caliber and funding that spurred lubrication technology into the modern age [1].

Advancements were made in bulk fluid properties, namely viscosity-temperature profiles, and upper temperature limits, and in specific additive formulations such as anti-wear and extreme-pressure. Development of petroleum derivative oils, synthetic base stocks, and additives that are more specific in function continued following the war effort in industrial, military and commercial sectors. Focus was necessarily on lubrication of metallic, particularly ferrous, substrates as these dominated most applications. Mid-twentieth century developments in ceramics as structural materials promoted investigations into the tribological properties of friction and wear of these materials.

## **2.2 Ceramic Applications**

The characteristics of ceramics and applications for which they are being applied are summarized in Table 2.1. The potential for ceramics and the importance of developing tribological systems capable of reliable operation are most obviously connected in the design of the low-heat rejection or so-called “adiabatic” engine. Ceramics have been selected for their thermal and/or tribological properties in several roles to extend the operating temperatures of these engines, and to reduce cooling and inertial loads. The ceramic diesel engine offers substantial economies in efficiency, durability and power-to-weight ratios. Katz estimated a possible fuel savings with the application of ceramics on the order of \$ 5 billion in the US alone [2].

**Table 2.1 - Ceramics in Tribology**

<u>Characteristics</u>	<u>Applications</u>
<ul style="list-style-type: none"><li>• High thermal stability</li><li>• Chemically inert</li><li>• Low thermal conductivity (most)</li><li>• Good abrasive/erosive wear characteristics</li><li>• Low density</li><li>• Low thermal expansion</li></ul>	<ul style="list-style-type: none"><li>• Cutting tools</li><li>• Low-heat rejection engines</li><li>• Replace existing engine components</li><li>• High performance turbomachinery</li><li>• Magnetic recording heads</li></ul>

The excitement over the promise of ceramic based adiabatic (low heat rejection) engines initiated ceramic heat engine programs in the US. Bratt [3] stated the implications of such programs as follows.

If ceramic engines contact surfaces do operate at temperatures near to 1000 °C , as opposed to only a couple of 100 °C, then entirely new lubricant systems will actually be required. It will necessitate major lubricant development programs, perhaps comparable in scope to the ceramic heat engine program itself. ... Wear problems, particularly whenever moving ceramic and metallic parts are in direct contact, will provide for additional problems and certainly push lubricants to well beyond their current limits, particularly their upper level temperatures of performance.

Although the extreme temperatures mentioned above can never be sustained by organic based liquids, other components of the proposed engine would operate at much lower temperatures and offer durability, dimensional, and weight advantages. In addition, the promising results of vapor phase lubrication using the tribopolymerization approach will aid in bridging the gap between the liquid thermal limits and the temperature ultimately

required for ceramic engine applications. Furthermore, ceramic lubrication developments are in demand at lower temperatures for some reasons already mentioned: cost savings based on weight, maintenance and durability economies provided by ceramic wear resistance, and applications to existing engine technology thermal demands.

Several patents claim methods for increasing wear resistance of ceramics, thus reducing the burden of conventional lubrication. One of these roles incorporates wear resistant coatings on ceramics as described in U.S. Patent 5139876 “Ceramic article having wear resistant coating [4].” Chemical deposition of activating metal ions (on ceramic) followed by deposition of an adherent organic polymer film on the activated surface is claimed to offer resistance to mechanical wear at temperatures of 500 °C and higher. A second role for ceramics is described in U.S. Patent 5413877 “Combination thermal barrier and wear coating for internal combustion engines [5].” In this case, a thermal barrier material layer of ceramic is initially applied to the friction-bearing chamber wall surfaces of an internal combustion engine followed by a second self-lubricating wear layer. The combination is claimed to be able to withstand temperatures up to 900 °C.

To successfully apply ceramics to an end use, many manufacturing and durability issues are being explored. Success is in the near future as Isuzu Motors has been awarded a patent for a ceramic engine [6]. The engine consists of a ceramic cylinder liner, ceramic portions of connecting rods, suction ports, and is powered by alcohol fuel. These successful applications of ceramic materials will promote increased fuel-efficiencies and can be further supplemented with new approaches to lubrication as demanded by the tribological and tribochemical characteristics of ceramics.

In light of these promising developments however, the conventional role of the lubricant in a tribological system will likely continue. The lubricant is an essential element in providing a durable tribological system as it removes contaminants, harmful wear byproducts and heat while supplying hydrodynamic and boundary lubrication to whatever material interface the engineer desires. Some of the conventional methods of ceramic lubrication are discussed next.

### **2.3 Conventional Ceramic Lubrication**

It has been widely recognized that a fundamental limitation in using ceramics in the boundary lubrication (BL) regime is the relative chemical inertness of such substrates. Although this characteristic of ceramics has the advantage of mitigating corrosive or other chemical processes that can cause friction and/or wear, it is disadvantageous to the formation of tribochemical or chemisorbed anti-wear films through reaction with the surface. Used extensively in metallic systems, common BL additives such as zinc dialkyl dithiophosphate (ZDDP) [7,8], fatty acids and alcohols [9-13], and tricresyl phosphate [14,15] were found less effective for ceramics. Although the effectiveness of each additive varied with respect to various ceramics, Habeeb et al. [7] found only a negligible effect of the most common boundary lubricant additive, ZDDP, in the alumina system. Most of the existing additives are present in the boundary regime due to surface phenomena such as physisorption and chemisorption if not chemical reaction. The mechanism of tribopolymerization however, is well-suited for boundary lubrication of ceramics primarily because chemisorption and chemical reaction with the surface are theorized to be unnecessary.

## **2.4 Recent Developments in Ceramic Lubrication**

The summary of the state of the art in ceramic lubrication is based on a review of recent patents and literature. Without physically altering the ceramic itself with a coating or surface treatment, wear protection and the reduction of friction are accomplished with various lubricants and systems of delivery to the contacting areas. The patents are organized by phase of lubricant and their applicable temperature ranges. The patents reviewed span from Habeeb 1989 to Wedeven in December of 1996. A summary of the essential elements of claims made within these representative patents follows.

### ***Liquid Based Lubrication***

Habeeb's patent [16] describes a method using oxidants such as hydroperoxides in a lubricating oil to reduce wear for ceramics on ceramics or metals. Examples of such hydroperoxides are, cumene hydroperoxide, tert-butyl hydroperoxide, and possibly superoxides. His claims included lubricants with and without zinc dialkyldithiophosphate. Contacting conditions were claimed to be between 20 and 150 °C with pressures between 80 to 350 kPa. Concentrations ranged between 0.01 and 2.5 %. However, the presence of metals in lubricant molecules presents an environmental hazard.

Wedeven's patent [17] "Method for broad temperature range lubrication with vapors" solves the compromise between high temperature lubrication and low temperature flow. Lubricants used consisted of a range of molecular weights of perfluoroalkylpolyethers (PFPE's) selected based on vaporization temperatures. These lubricants must not yield solid decomposition products nor autoignite within the range of temperature operation of the contacting surface. A small amount of fluid is provided to

uncooled surfaces where it condenses and provides elastohydrodynamic lubrication (EHD). The temperature ranges claimed are between 350 and 670 °C with lubrication above 500 °C assisted in the boundary regime by extreme pressure additives such as tricresyl phosphate. One drawback of this approach is the requirement for separate heating of the lubricant to its vapor point and beyond and subsequent collection of the condensate. A major challenge for this approach could be effectively supplying lubricant to the piston/cylinder area.

### ***Lubrication by other phases***

Rosado's patent "Lubrication by sublimation" [18] describes a system and method for high temperature lubrication of a bearing surface. Thermal contact with a heater sublimates a solid lubricant producing lubricant vapors, which are conducted to the bearing surface via conduit. The patent claims several suitable solid lubricant groups such as cesium oxythiotungstenate, molybdenum disulfide, tungsten disulfide, zinc oxythiomolybdate, and cesium oxythiomolybdate. The solid lubricant is heated in excess of 800 °F (427 °C) and operating temperatures are claimed between 800 and 1300 °F (427 and 700 °C). The test material was silicon nitride and the geometry was ball-on-rod rolling contact fatigue. Heating and supply of the solid lubricant are difficulties associated with this approach.

Lauer [19] discusses high temperature lubrication, (450 to 650 °C) using carbon deposited by surface reaction of carbonaceous gases (ethylene) as a means of enabling low heat rejection engines. The wear reducing carbon film was found to stick tenaciously

to the Sialon surface. Lauer later explains a carbon lubrication method using gases made to pyrolyze at temperatures above 700 °C. Here the carbonaceous films were identified as diamond and graphite like. A similar mechanism was described by Ashley [20] consisting of injecting a stream of hydrocarbon bearing exhaust gases into a ceramic engine's bearings and friction surfaces. Similar to Lauer's mechanism, the hydrocarbons in the gas will turn into a coat of graphite-like carbon lubricant. The speed of reaction and formation of these protective carbon films may be a limiting factor in practical applications. However, these methods show high-temperature feasibility and may replace or supplement recent developments in liquid phase lubrication.

Regardless of the method of lubrication, indeed if any is used at all, one element consistent in all tribological design solutions remains. This element is understanding the wear mechanism(s).

## **2.5 Ceramic Wear Mechanisms**

If successful high temperature lubrication of ceramics is to be systematically achieved a fundamental key of the design effort must be an understanding of the mechanisms by which ceramic material is removed in tribological contact. A fundamental difference in the contact mechanics of ceramics and metals is the lack of gross plastic deformation of the former. Brittle fracture of ceramic asperities leads to removal as microcracks propagate until complete separation of debris results. Braza [21] attributed modes such as chipping, spalling and grain pull out to intergranular and transgranular brittle fractures.

Ceramics have short critical crack lengths that lead to very fine wear debris. Jahanmir [22] observed debris in the contact region that had chemical structure

differences in comparison to the bulk. Debris entrapment between asperities, development of aluminum hydroxide interfacial layers, and formation of aluminum monohydroxides (in alumina systems) have all been proposed as controlling wear mechanisms involving post-partum ceramic debris. The formation of a sacrificial interfacial film that reduces the severity and degree of contact is the intended anti-wear mechanism for tribopolymerization. Tripathy [23] noted the significance of debris interaction in tribopolymerization studies on alumina systems stating that wear reduction was associated with a compact layer of wear debris found on the surface using scanning electron microscopy (SEM).

Although the approach under study was initially applied to ceramics because of its potential with unreactive substrates, tribochemical reactions of lubricants *with* ceramic surfaces may also play an important secondary role. Thus, the design of lubricant additives must take into consideration the following tribochemical interactions:

- (1) ceramic substrate  $\Leftrightarrow$  additive (e.g. surface energy, physical/chemical adsorption)
- (2) ceramic debris  $\Leftrightarrow$  additive (e.g. friction/wear/stress activated sites)
- (3) ceramic substrate  $\Leftrightarrow$  lubricant  $\Leftrightarrow$  additive (e.g. competition between polar ester synthetic lubricant and polar additive)
- (4) ceramic debris  $\Leftrightarrow$  lubricant  $\Leftrightarrow$  additive (same as (3))

Careful investigation of boundary lubrication additives requires consideration of all factors before concluding an anti-wear mechanism and/or utility.

Ceramics can withstand higher contact pressures, higher temperatures and more severe chemical environments. The combination of these three factors can make the tribological boundary interface a hot zone for tribochemical changes. Thus, an approach

that takes advantage of this high boundary energy environment would be a prime candidate for study on such systems. Such is the case for *tribopolymerization*.

## 2.6 Tribopolymerization

The tribopolymerization concept, originally proposed by Furey [24, 25] and later updated by Furey and Kajdas [26-35], is formally defined as:

The planned or intentional formation of protective polymeric films directly and continuously on rubbing surfaces to reduce damage and wear by the use of minor concentrations of selected compounds capable of forming polymeric films *in situ*.

The cornerstone of this novel approach lies in taking advantage of the energy conditions at the contact interphase to promote anti-wear films from the monomer additives. A brief summary of the development and history of tribopolymerization is presented next. A more detailed review is given by Tripathy [23].

Initial laboratory testing involving a long-chain C<sub>36</sub> dimer acid/ethylene glycol derived monoester in the Ryder Gear test (metal) [24] showed great promise as an anti-scuff additive with the military jet fuel JP-4. Anti-scuff ratings increased to 5200 N/cm from 350 N/cm with the addition of the monoester. Subsequent field testing in aviation jet fuel pumps of this tribomonomer yielded great wear reductions. A V-8 automotive engine valve train wear test using a mineral base oil containing 1 wt % of C<sub>36</sub> dimer acid/ethylene glycol monoester demonstrated viability in such systems [36]. As measured using radioactive valve lifters, the tribomonomer additive reduced wear by over 90%.

The anti-wear mechanism was investigated by comparing the addition of preformed polymer versus the potential *in situ* polymerizing monomer. This work

indirectly supported the novel mechanism of tribopolymerization as the preformed polymer failed to function nearly as effectively as the monomer additives. The use of Fourier transform infrared spectromicroscopy (FTIRM) yielded the first direct proof of the mechanism as Marin-LaFleche, Furey, and Kajdas found characteristic polystyrene spectra on a fretting wear surface lubricated with a base fluid containing a small percentage of styrene as additive [35,37-38]. Smith [39], Tripathy [23] and Tritt [40] found similar FTIRM evidence of tribopolymerization. Smith's studies involved vapor-phase delivery of the monomers in a nitrogen carrier to an alumina interface while Tripathy's investigated temperature, load and speed effects. Tritt's looked at the effects of high load and high speed. Their research set the precedent for this investigation and is discussed next.

For polymerization to occur an initiation step is needed for both condensation and addition reactions. This initiation, necessarily *in situ*, was hypothesized to be elevated temperature for the condensation (step) pathway and free radical generation via triboemission of exoelectrons for addition (chain) polymerization. Low thermal conductivity of ceramics leads to higher surface temperatures due to the decreased heat flux away from real areas of contact. Studies of materials with and without exoelectron emitting properties found exoelectron emission an important variable in wear reduction. Alumina has been observed by Nakayama [41,42] to emit exoelectrons. Thus, initiating mechanisms are present in certain ceramics for both pathways to polymerization. This led to in depth studies of the lubrication approach for use with alumina. Tripathy [23] tested five addition and one condensation monomers in alumina-on-alumina pin-on-disk tests. All were found to reduce wear rates at a load of 20 N and velocity of 0.250 m/s.

Varying the velocity was found to have diverse effects on the lubricant additives wear reductions compared to the reference fluid. Load variation revealed an improved wear reduction with increasing loads although extensive loads were not tested. Tripathy suggested that the improved performance was due to higher temperature. Subsequent investigations that varied bulk lubricant temperature found each monomer to have distinct temperature related anti-wear effects. Most interesting of the effects was the striking decrease in wear between 50 and 150 °C for the nitrogen containing compound methyl-2-acrylamido-2-methoxy acetate (MAMA). At 100 °C this compound reduced wear by a remarkable 98 %. An important side note is that Tritt's work, discussed next, showed no significant anti-wear behavior for MAMA at high-speed or high-load

Tritt [40], using a machine originally designed by Smith [39] investigated the effectiveness of the same group of monomers under a 2x2 matrix of loads and speeds representing a theoretical surface temperature rise of 16 fold. The results of his study indicated, surprisingly, that speed was the limiting factor. A summary of his results combined with Tripathy's at low speed and various loads is shown in Figure 2.5.1. It can be seen that there is a general trend in improved anti-wear effectiveness at higher loads. However, these anti-wear compounds were clearly ineffective at the high speed (1.0 m/s) at both loads of 40 and 160 N. Tritt proposed that the effective range of surface temperature rise for tribopolymerization might have been exceeded. Based on these results, further research was suggested aimed at finding the actual range as well as finding more thermally stable compounds that may be effective beyond the limits suggested by his study. Smith tested three vinyl (containing a carbon double bond) monomers with the same pin-on-disk device as Tripathy with modifications for vapor

phase experiments. He found that temperature was an important factor in the anti-wear effectiveness of these compounds. Higher temperature led to greater wear reduction with respect to the nitrogen reference.

In summary in relation to this effort, MAMA, containing nitrogen, showed an optimum anti-wear effect at 100° C (Tripathy). At the same time, MAMA was ineffective at any load with the sliding speed of 1.0 m/s. The monoester and diallyl phthalate showed good anti-wear behavior at low and high loads at 0.25 m/s (Tritt) and improvement of anti-wear behavior with increasing load at low speed (Tripathy). Finally, vinyl monomers increased anti-wear behavior with increasing temperature in the vapor phase under a nitrogen environment. How will the new anti-wear additive classes of this study behave? And under the increased frictional heating of higher loads and speeds?

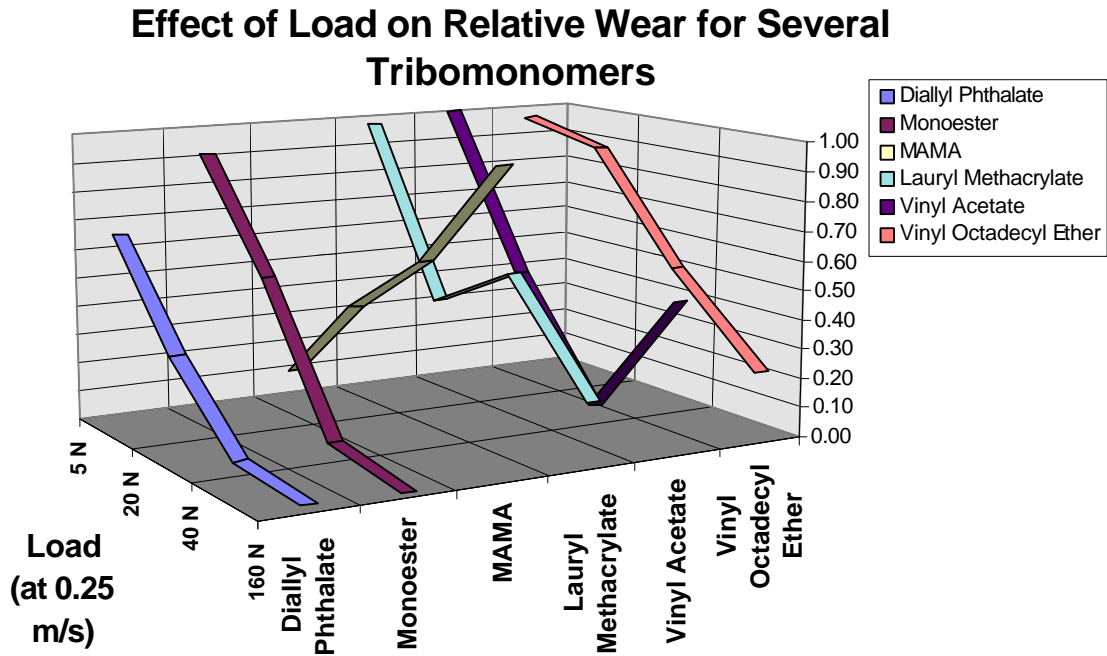


**Figure 2.5.1** Effect of Load on Relative Wear for Several Tribomonomers

## 2.7 High-temperature monomer additives.

Polymerization is a complex chemical reaction and an in depth analysis of the factors affecting even one phase of the process for one particular polymer is beyond the understanding of the author. However, several general observations are relevant to the design of the desired high temperature ceramic lubricant additives. First and most importantly is the functionality required for polymerization to occur. A functional group is part (usually an end or branch) of a molecule that gives it a characteristic chemical trait. For example, the -OH group attached to a hydrocarbon chain (designated R) is characteristic of an alcohol. Reaction with an acid group -COOH, yields the condensation product H<sub>2</sub>O and an “ester”. This is precisely the chemistry of the successful tribomonomer C<sub>36</sub> ethylene, glycol monoester. Combination of these two different species is in general described as an A-R-B link. Polymerization occurs when an A-R-B compound, or two compounds A-R-A + B-R'-B, is (are) present in conditions sufficient for them to initiate and propagate a polymerization reaction. If a byproduct is condensed the reaction is called, naturally, a condensation reaction or often a step reaction. Where joining of functional groups is accomplished without the evolution of a third chemical body, the reaction is described as a chain-reaction or addition type. A third, previously unexplored mechanism of antiwear tribopolymerization reaction, is the “ring-opening” polymerization. This reaction occurs when the chemical thermodynamics are sufficiently favorable for a cyclic structured organic compound to uncoil at a particular site and then reattach in a linear arrangement forming a long chain of the former monomers. This mechanism is a path by which caprolactam forms one of the familiar Nylon series of polymers.

Thus, fundamental tribopolymerization mechanism anti-wear design of additives involves the initial selection of appropriate functional groups sufficient to form these macromolecules. The type, number and location of these functional groups are additional design variables to be considered once the fundamental minimum chemical structural characteristics have been met. All polymerization reactions share the general sequential steps of initiation, propagation, and termination. Type, number, and location of functional groups, along with hydrocarbon chain length influence the individual trademarks of a monomer's three steps in the polymerization process. Other non-chemical factors such as concentration (initiator/inhibitor/monomer), temperature, pressure, and catalysis play an integral role in typical polymerization reactions. Non-molecular additive factors varied to date for tribopolymerization experiments have included the substrate, operating conditions (load, speed and temperature), concentration, and carrier fluid. Although additives to date have not been specifically designed to suit any of these factors the following general observations influence the criteria for selection.

1. Monomer additive solubility in carrier fluid is considered essential with higher solubility desired.
2. Reactivity with the substrate is desirable for initiating polymerization on the surface after chemisorption or strong physisorption, or mere adsorption: however it is not theorized to be critically necessary.
3. The combined load and speed effects on frictional heating should be sufficient to thermally activate polymerization given the operating bulk temperatures of the given system. (Note that substrate hardness and thermal properties, carrier fluid, and system design all contribute).

4. Molecular properties such as functional groups of nitrogen, oxygen, and cyclic rings tend to give the formed films better anti-wear performance at higher temperatures.

In summary, evidence supporting the mechanism and recent results using tribopolymerization guidelines has reinforced the value of this anti-wear approach. The thermal ceiling has yet to be firmly established and additives, which promise higher thermally stable films, remain to be tested. With respect to any particular tribopolymerization additive, questions remain as to the individual and combined effects of surface chemistry, surface temperature, pressure, loads and sliding speeds.

## Chapter 3

# EXPERIMENTAL

### 3.1 Introduction

A pin-on-disk geometry was used for tribological testing of the new classes of anti-wear additives. To test the new lubricant molecular structures, various compounds were mixed at low concentrations in a relatively inert organic carrier fluid. Test specimens consisted of complimentary ball and disk material pairs made of steel and two distinctly different hot-pressed aluminas. Stylus profilometry and photomacrography were used to compare the quantitative and qualitative effects of additives on wear with respect to the carrier reference. Surface analytical techniques were employed to identify tribochemical changes on and near the worn areas. This chapter describes the equipment and procedures used over the course of the exploratory research study.

### 3.2 Pin-on-Disk Device

The pin-on-disk device designed and assembled by Smith [39] was later modified by Tritt [40] and then the author. The design consisted of specimen holders and load application apparatus fitted to a milling machine that provided variable sliding speed. The ball was secured to a lubricant cup on an assembly mounted to a linear spline bearing supported by the X-Y table. An upward force from the pneumatic pancake cylinder was applied through the spline-bearing-ball-holder assembly moving it vertically into contact with the disk. The disk was mounted in a holder assembly attached to the rotating shaft. Speeds were adjusted by changing track radius and speed of rotation. The track radius was controlled by moving the ball relative to the centerline of the milling machine shaft using the X-Y positioning table. Load control was afforded using feedback from a strain

gauge type force transducer mounted in-line between the spline-bearing and pneumatic cylinder. The normal load was calibrated using known weights. Changes made by the author included adding data acquisition of the normal load signal from the strain gauge box and modifications to better allow entrapped air to escape the inverted ball-on-disk geometry.

### 3.3 Tribological Materials

For the steel system tests, disks were cut from a 25 mm (1 inch) rod and finished by the Mechanical Engineering Shop of Virginia Tech. Steel ¼ inch ball bearings were purchased from a vendor. Two alumina material systems were used, a system being defined as a set of ball and disk materials. The alumina balls used in both ceramic systems came from a single lot order and showed similar wear patterns. The alumina ball specifications ordered from Sapphire Engineering were 99.5% pure, Grade 25 balls of size 6.35 mm (1/4 inch). Both systems disks were ordered from LSP Industrial Ceramics with order specifications for 99.5% pure isostatically pressed alumina rod cut to 3.2 mm thick and ground to an average surface roughness of 0.5-0.65 µm (CLA). The first, Alumina “A” System disk specimens remained from a previous lot. A new batch of disks of 100 specimens, Alumina “B,” was ordered and had distinctly different wear characteristics and visual appearance. Table 3.1 gives statistics for the three systems.

**Table 3.1 Test Specimens**

Specimen Material Property/Statistic	Disk Material		
	Steel	Alumina A	Alumina B
Total Specimens	26	18	>50 (both sides used)
# Reference Tests	16	6	> 30
Reference Average <sup>1</sup>	0.84 mm <sup>3</sup>	27.1 mm <sup>3</sup>	1.73 mm <sup>3</sup>
Reference Range <sup>1</sup>	0.04 – 3.36 mm <sup>3</sup>	6.6 - 50 mm <sup>3</sup>	0.22 – 2.32 mm <sup>3</sup>

<sup>1</sup>Total Wear Volume

### 3.4 Lubricants

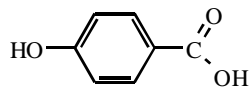
Three new classes of tribopolymerization additives were tested in solution or mixture at 1% or less by weight in hexadecane. The classes included A-R-B type condensation monomers, A-R-A with B-R'-B in molar combinations, and cyclic amides. As a separate study, some A-R-A and B-R'-B compounds were tested alone. Molecular structures are given in Figure 3.4.1. The oxydianiline (ODA) and benzophenone-tetracarboxylic-dianhydride (BTDA) compounds were donated by Polymer Solutions of Blacksburg, Virginia. Chemical suppliers for other compounds included Aldrich Chemical and Kodak. The carrier fluid was hexadecane with a minimum purity of 99% obtained from Aldrich. All of the compounds were partially soluble up to 40 °C, with the exception of caprolactam and lauro lactam, which both completely dissolved after an hour of gentle stirring. Upon cooling, the solutions from the lactams readily recrystallized. Shaken at room temperature, all of the other mixtures were cloudy white with particulate size dependent on consistency of the dry compound. Two compounds, a monoester and diallyl phthalate, were tested for comparison to earlier studies. These were miscible liquids at 1% concentration in hexadecane. Additional information on these additives from earlier studies can be found in the works of Tripathy [23] and Tritt [40].

# NEW TRIBOPOLYMERIZATION MOLECULAR CLASSES AND STRUCTURES

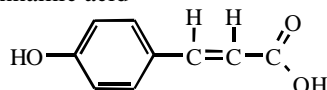
## (1) A-R-B COMPOUNDS

### Aromatic Hydroxy Acids

4-Hydroxy benzoic acid

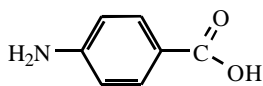


4-Hydroxy cinnamic acid

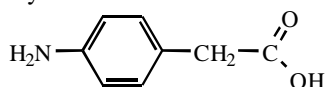


### Aromatic Amino Acids

4-Amino benzoic acid

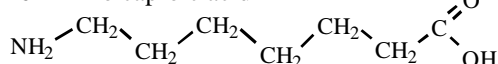


4-Amino phenylacetic acid



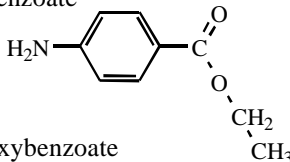
### Paraffinic Amino Acid

6-Amino caproic acid

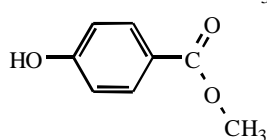


### Aromatic Amino Esters

Ethyl-4- Aminobenzoate

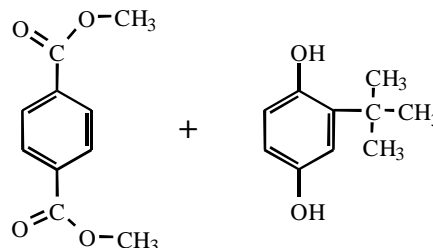


Methyl-4- Hydroxybenzoate



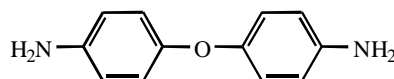
## (2) A-R-A + B-R'-B COMBINATIONS

Dimethyl terephthalate\* + tert-Butyl hydroquinone

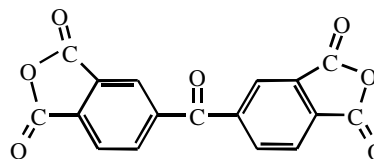


### *DuPont's Kapton monomers*

4,4'-Oxydianiline (ODA)

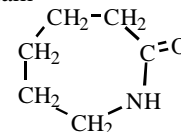


+  
3,4,3'4'-Benzophenone tetracarboxylic dianhydride

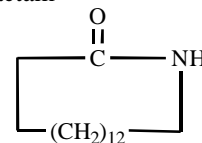


## (3) CYCLIC AMIDES

Caprolactam



Lauro lactam



\*Compounds also tested alone, dimethyl phthalate isomers not shown.

**Figure 3.4.1** New Tribopolymerization Molecular Classes and Structures

### 3.5 Procedure

Material specimens were cleaned in successive 10-minute ultrasonic baths of acetone, methanol, and hexane, then dried in a vacuum oven at 250 °C at 25 mm Hg vacuum before sealing in Teflon lined jars for future use. Before each experiment test equipment that contacted the lubricant was wiped, cleaned in 10 minute ultrasonic baths submerged in methanol and then hexane, and then dried with a low-lint chemical napkin. In preparation for each test the strain indicator was turned on and Amp zeroed for 10 minutes. Meanwhile, a new cleaned disk was labeled then installed into the stainless housing and screwed onto the mill chuck. A cleaned ball was set in position using tweezers, then tightened into the ball holder, which then screwed into the ball-spline bearing through the lubricant cup. For high-speed tests, a splash guard formed from a cleaned aluminum soda can top was fitted over the lubricant cup such that the rotating shaft passed through the hollowed out rim. This countered the overflow of lubricant typical of stirring induced vorticity within the cup. After positioning the ball into vertical proximity of the disk using the milling machine Z-elevator, the load was applied. Pressure to the pneumatic pancake cylinder was increased forcing the ball assembly up through the spline bearing until a strain reading corresponding to a 40 or 80 N normal load was obtained. With the materials in contact and the load applied, sliding was initiated by starting rotation of the milling machine. The test was timed to correspond with the set sliding speed to allow a sliding distance of 250 m. Minor adjustments to the pneumatic pressure were made throughout the test periodically to maintain the desired average strain indicator reading.

The tests were ended in sequence by hitting the emergency stop button, decreasing the pressure, and lowering the table in rapid succession. The specimens were removed from the device for sample analysis. The wearing of latex medical gloves at all times during handling of specimens minimized contamination by sebum (finger oils).

### **3.6 Sample Analysis**

Photomicrographs were taken of test specimens using a Leitz-Wild Photomicroscope. As necessary, rinsing with various solvents removed excess hexadecane and loose debris from the ball and disk areas. Measurements of the major and minor diameters of the ball wear area yielded an average which was then used to calculate the volume worn from the missing spherical segment. In the Steel and Alumina A systems, this assumption based on a flat circular ball wear area can only be loosely argued as evidenced by the non-circular ball wear areas in photomicrographs of these in Chapter 4. However, the calculation gives a conservative estimate as the major diameter reflects more surface damage than actual material removal. Combined with the small relative proportion of ball wear volume to total wear volume in these systems, this simplifying assumption was justified. In the steel system, ball wear volume contributed less than 4% of the total wear volume. For the Alumina B system, the resulting ball wear areas were in fact flat and circular as seen later in Chapter 4. In this system, ball wear contributed an average of 26% of the total wear volume.

A Taylor-Hobson Talysurf profilometer provided stylus profiles of the disk surfaces for the first two material systems, Steel and Alumina A. Digital data acquisition of the trace voltages was captured using Global Lab software. Once a visual display was

available a short program written in Matlab accepted four data points across the trace input via mouse clicks. The program interpreted and averaged the segments before and after the wear trough yielding a reference datum from which wear areas were calculated. An Alpha-Step 500 Profiler made by Tencor was available for disk profilometry of tests starting in the Alumina B system. Comparisons were conducted on several Alumina A disks to reconfirm data taken with the former profilometry methods. In the event that plowing was evident, the displaced areas did not contribute to the wear volume. As a note, no plowing areas were observed with either ceramic system. Four orthogonal traces of the disk wear scar were averaged to calculate an average worn area, which was then multiplied by the track circumference to yield disk wear volumes.

XPS analysis was performed to yield molecular compositions at the ceramic surface using equipment from Virginia Tech Chemistry Department's Surface Analysis Lab and Mr. Frank Kromer's expertise.

## Chapter 4

# RESULTS

To explore the potential of these new classes of tribopolymerization additives, tests were conducted with candidates from the three classes of additives, 1) A-R-B, 2) A-R-A + B-R'-B, and 3) heterocyclic amides. Exploratory testing of compounds began with a steel-on-steel material system. Subsequent investigations followed with testing on ceramic pin-on-disk specimens. The ceramic system testing consisted of two distinct sets of alumina disk materials. The first alumina system, "Alumina A" resulted in large volumes of disk wear, where as the second system, "Alumina B" resulted in lower wear volumes. Ball wear remained relatively constant in both alumina systems.

The following sections present results from the hexadecane reference tests for each system followed by results from selected additive(s) tests. The results include comparison wear charts and photomicrographs. Some charts present averages of several wear tests for a particular additive. Appendix A contains a complete record of ball, disk and total wear volumes for each individual test. In-depth discussions of the quantitative data in the charts and qualitative visual results follow in Chapter 5.

### **4.1 Steel-on-Steel Tests**

Ideally tribopolymerization functions similarly irrespective of substrate material reactivity. Traditional anti-wear additives, however, require chemical interaction with a reactive substrate, e.g. iron or iron oxide. Due to low cost and specimen availability,

initial validation of anti-wear potential and behavior of these new tribopolymerization additives began with a steel-on-steel system.

#### 4.1.1 Hexadecane Reference

The results of reference testing are presented below, followed in Sections 4.1.2-4 with comparisons of each additive class to the average of the reference tests. Shown in Figure 4.1.1.1 are the hexadecane reference tests run at *standard conditions* of 0.25 m/s, 40 N, and 250 m sliding distance. The tests are plotted according to increasing total wear volume.

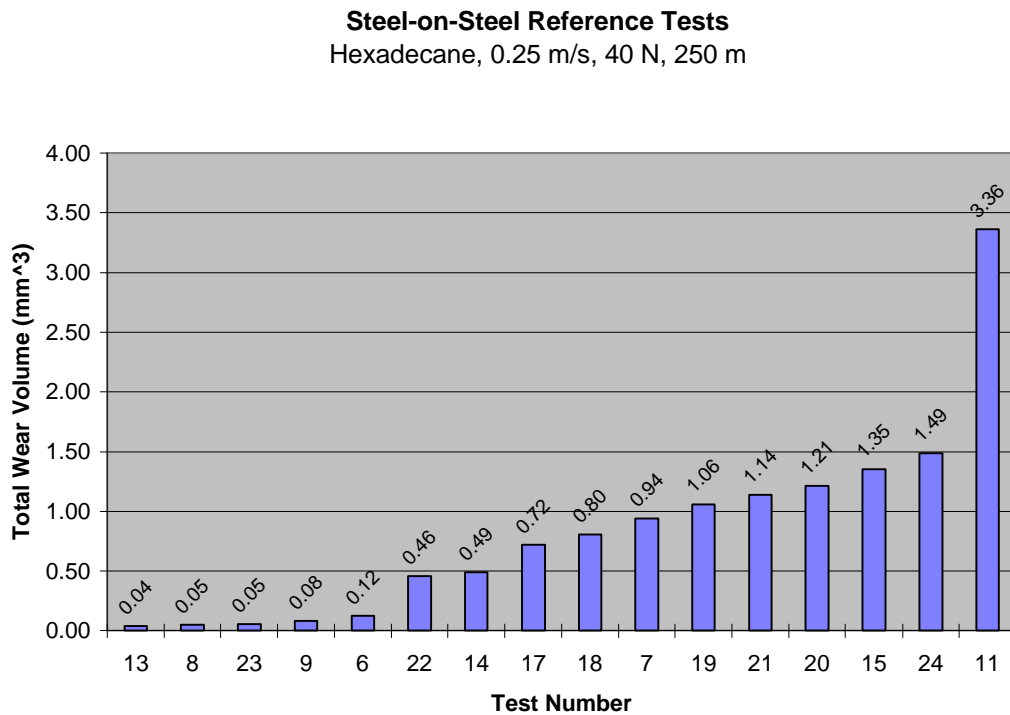


**Figure 4.1.1.1** Hexadecane Reference Tests in Order by Total Wear, Steel System.

The average total wear volume across the large range (0.04 to 3.36 mm<sup>3</sup>) for these sixteen reference tests was 0.84 mm<sup>3</sup> with a standard deviation of 0.836 mm<sup>3</sup>. The

following section compares additive test total wear volumes to this average. As mentioned in the previous chapter, disk wear contributed heavily to the total wear volume. Figure 4.1.1.2 shows the distribution of the ball percentage of total wear volume which ranged from 0.2 to 4.8 %.

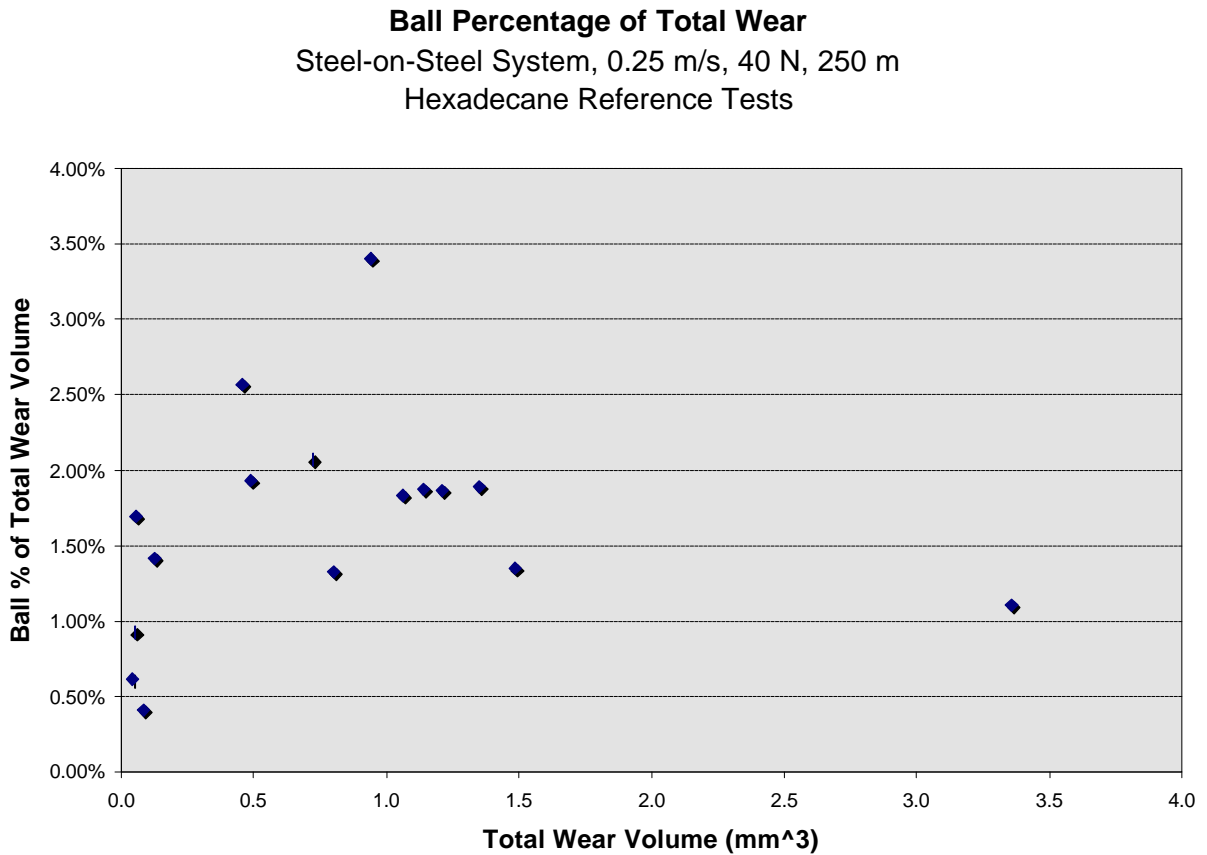


**Figure 4.1.1.2** Ball Percentage of Total Wear Volume for Hexadecane Reference Tests in Steel System.

Figure 4.1.1.3 presents a visual record of the nature of the diverse reference tests. All of the tests show evidence of severe adhesion and plowing with plastic deformation. Changes in lighting give some of the photos a blue tint. However, black wear debris was evident on some tests and not on others. It is believed that lubricant supply variations at

this stage of testing may account for the rinsing of some debris from some tests and not others.

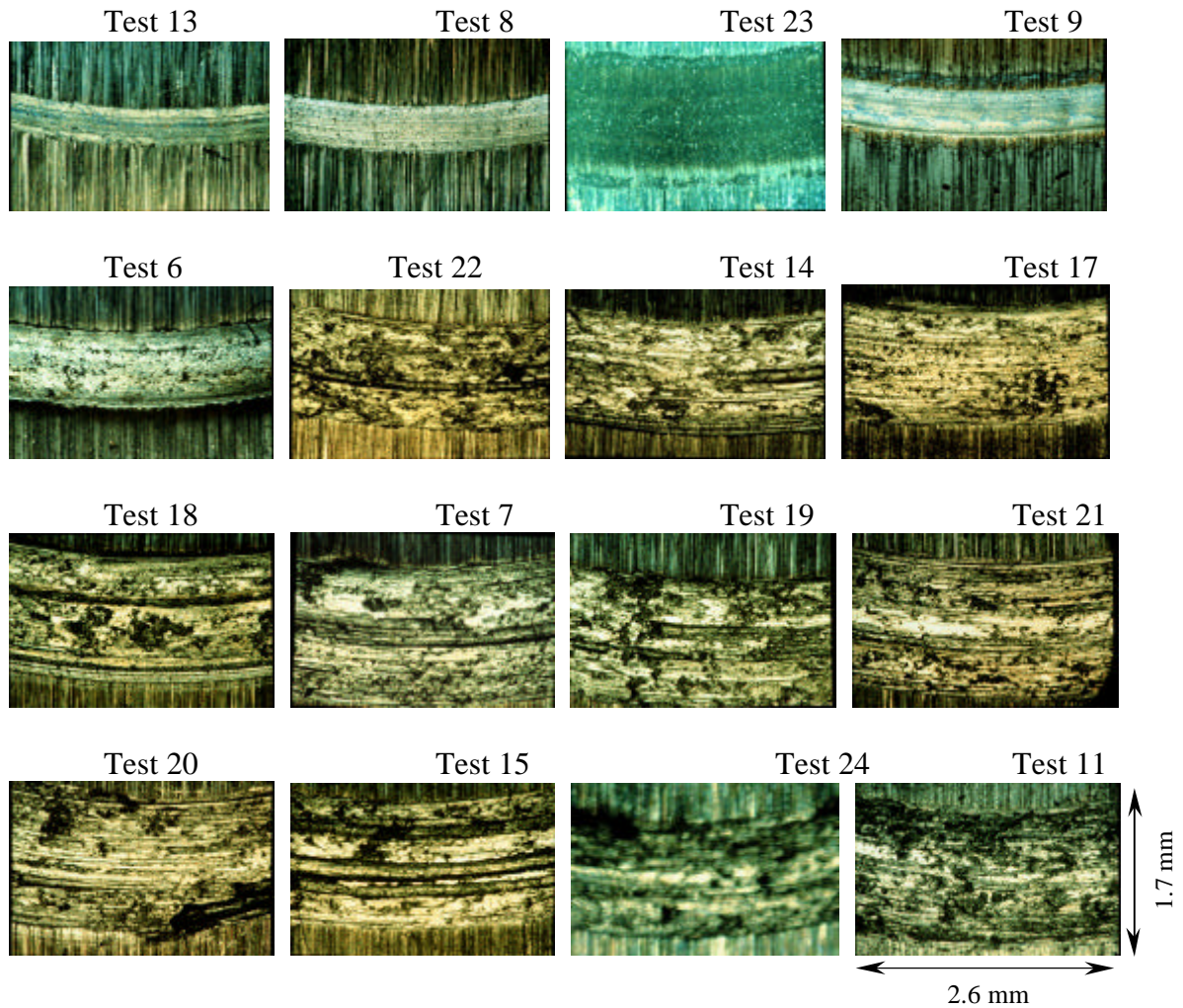


**Figure 4.1.1.3** Photomicrographs of Disk Wear Tracks for Hexadecane Reference Tests at 40x (All rinsed except Test 23)

#### 4.1.2 A-R-B Type Tribomonomers

Five new additives of the A-R-B class of tribomonomers were selected for evaluation at the 0.25 m/s, 40 N, 250 m [standard] test conditions. The first sub-group contained two aromatic hydroxy acids, 4-hydroxy benzoic acid and 4-hydroxy cinnamic

acid. The wear results in Figure 4.1.2.1 show the total wear (single tests) amounted to 58% and 96% respectively less than the reference average wear. Photomicrographs of the disk surfaces after testing show the usual adhesive wear mode for 4-Hydroxy benzoic acid in Figure 4.1.2.2 but strong attachment of dark wear debris on the 4-Hydroxy cinnamic acid test disk of Figure 4.1.2.3.

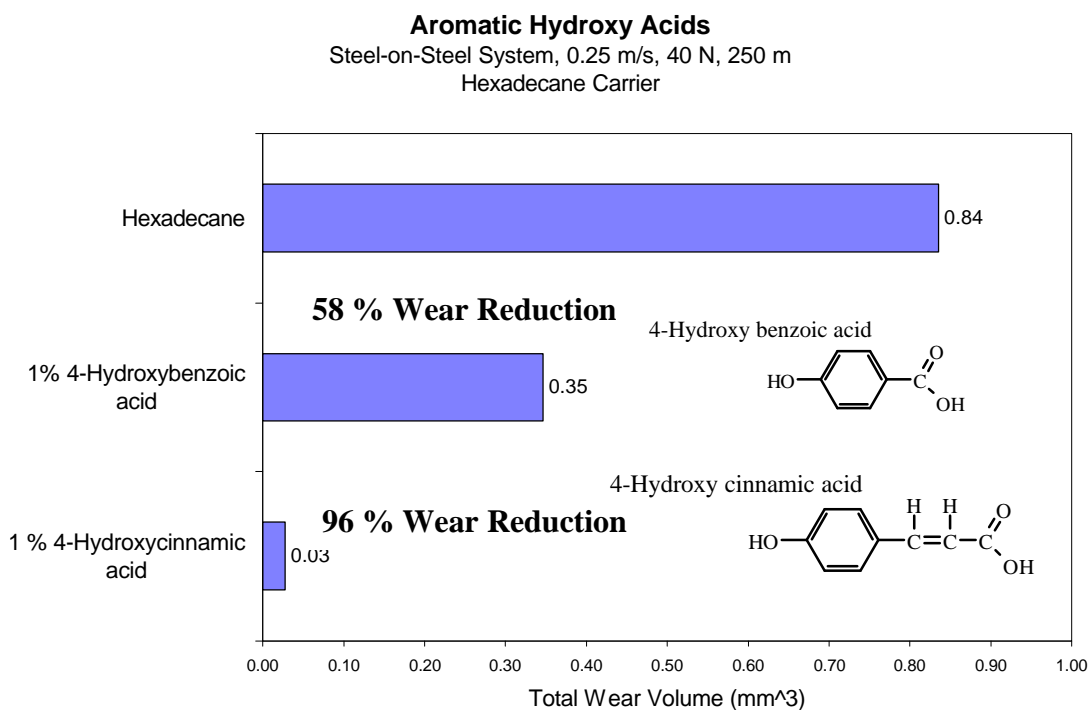


**Figure 4.1.2.1** Anti-wear Effects of Hydroxy Acids in Steel System.

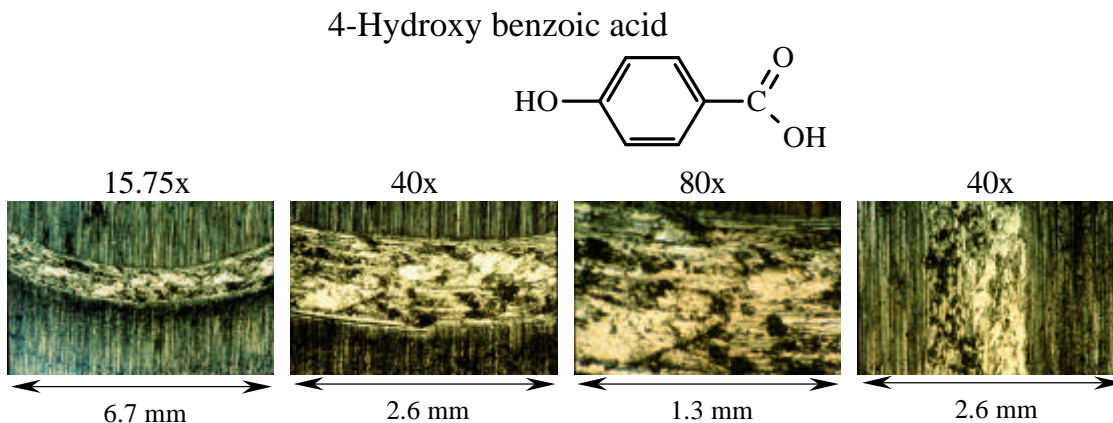


**Figure 4.1.2.2** Photomicrographs of 4-Hydroxy Benzoic Acid Disk Wear Track in Steel System (after methanol rinse).

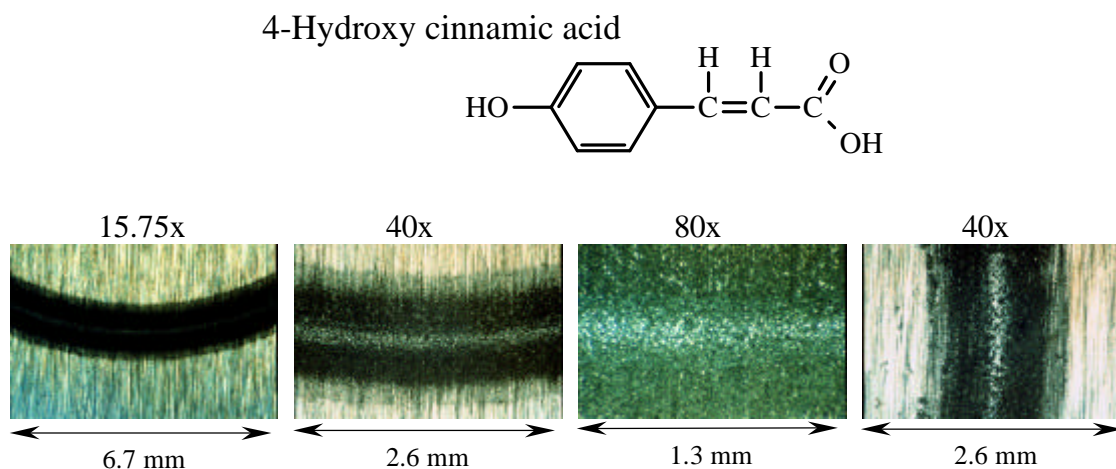


**Figure 4.1.2.3** Photomicrographs of 4-Hydroxy cinnamic acid Disk Wear Track in Steel System (after methanol rinse).

Figure 4.1.2.4 illustrate the effectiveness of single test results for additives from another A-R-B subgroup, the aromatic amino acids, which included 4-aminobenzoic acid and 4-aminophenylacetic acid. The photomicrographs of Figures 4.1.2.5 and 4.1.2.6 show interesting distributions of attached wear debris in and around deep dark grooves in the wear tracks.

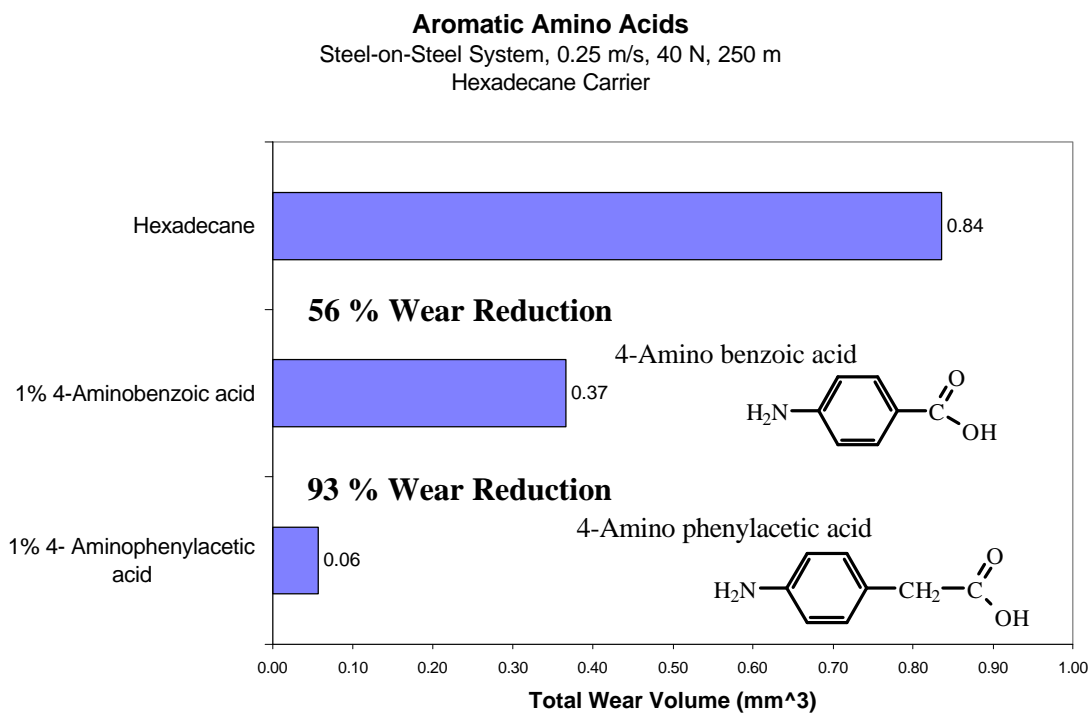


**Figure 4.1.2.4** Anti-wear Effects of Aromatic Amino Acids in Steel System.

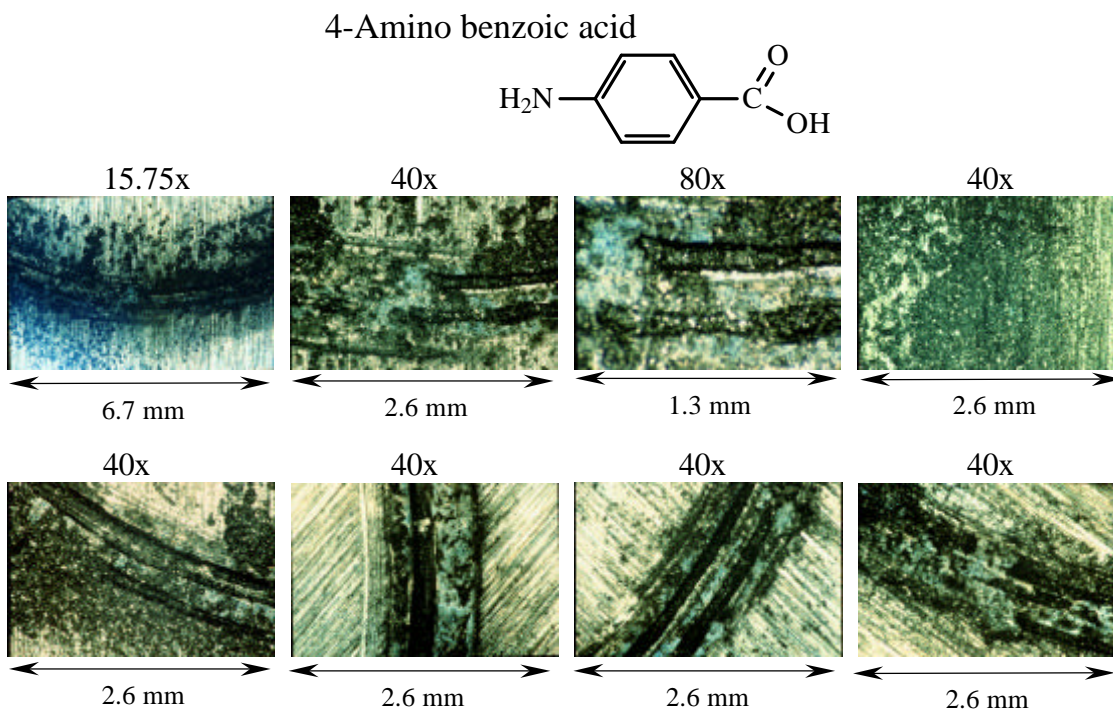


**Figure 4.1.2.5** Photomicrographs of 4-Amino Benzoic Acid Disk Wear Track in Steel System.

4-Amino phenylacetic acid

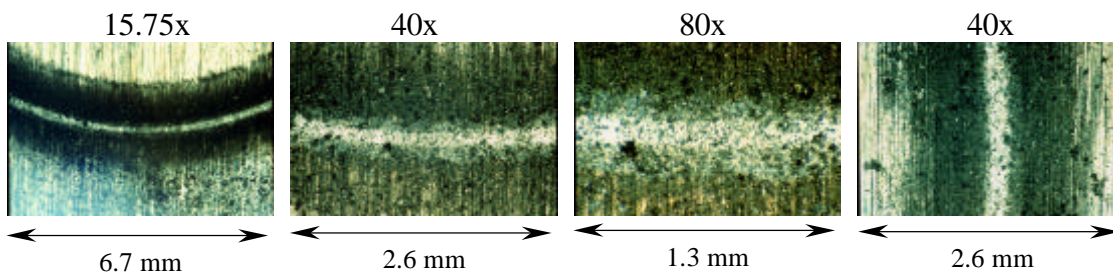
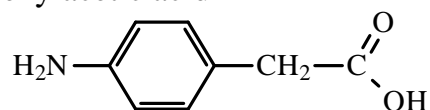


**Figure 4.1.2.6** Photomicrographs of 4-Amino Phenylacetic Acid Disk Wear Track in Steel System.

The aromatic amino acids were seen to effectively reduce steel wear. Replacing the acid end group with an ester group gave a similar wear reduction as evidenced by the result for the aromatic amino ester ethyl-4-aminobenzoate. Figure 4.1.2.7 shows the average of two tests for this compound compared to the reference average. The upper set of photomicrographs of Figure 4.1.2.8 shows the small degree of wear surface on the disk while the lower set demonstrates the unique pattern of fine wear debris resulting from an ethyl-4-aminobenzoate test.

The next class tested in the steel-on-steel system was the A-R-A + B-R'-B Type Compounds. Wear results and photomicrographs for these compounds are presented next.

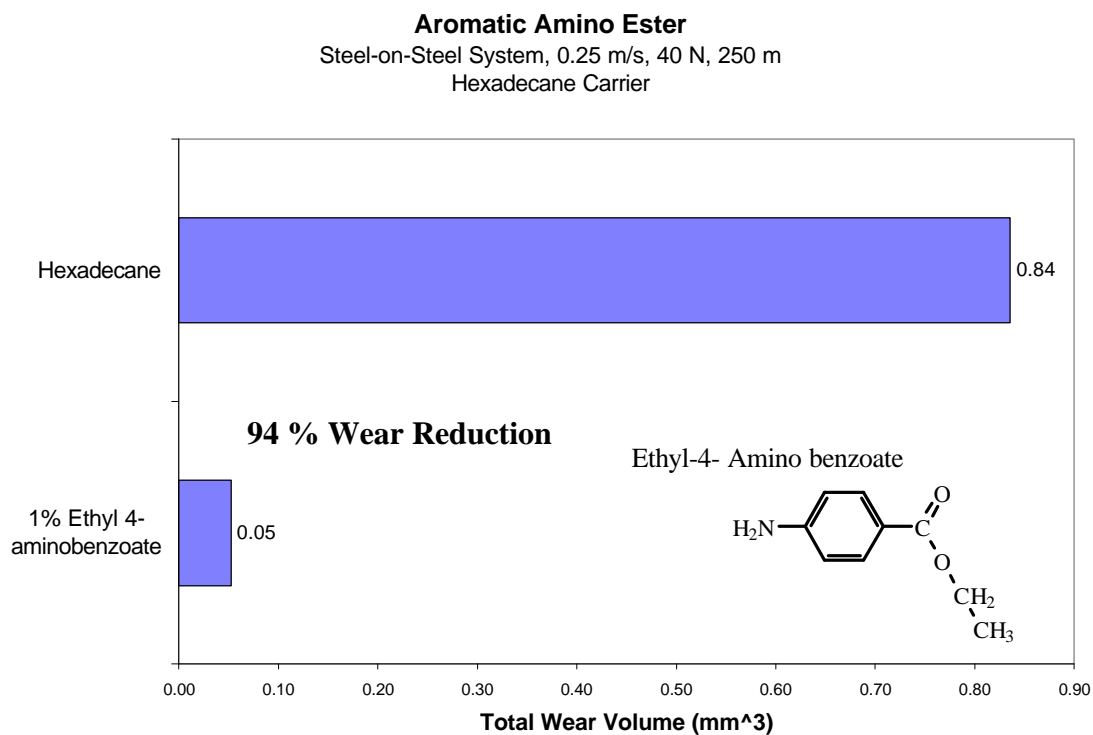


**Figure 4.1.2.7** Anti-wear Effect of Aromatic Amino Ester in Steel System.

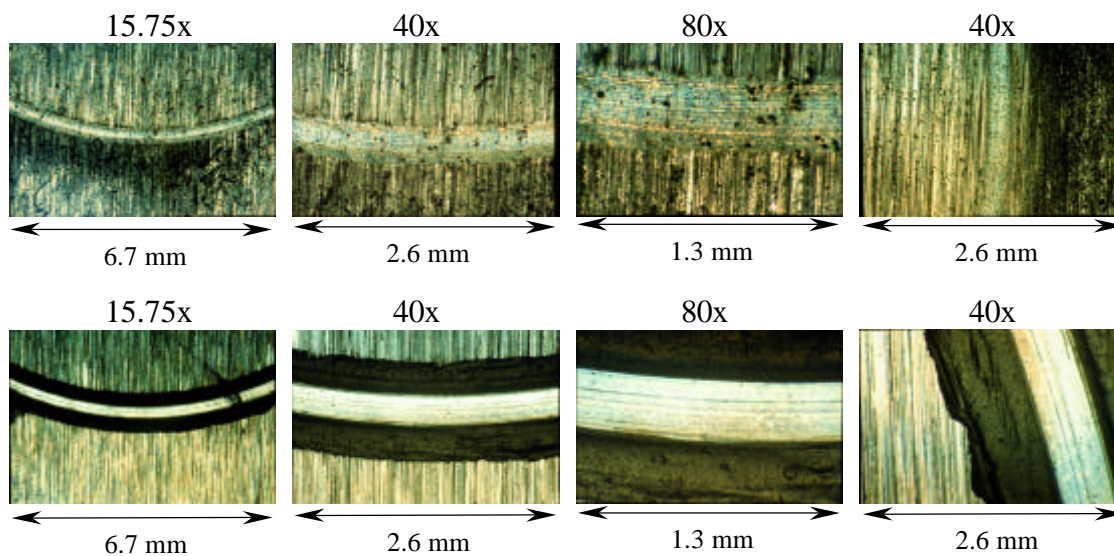


**Figure 4.1.2.8** Photomicrographs of Ethyl-4-Amino Benzoate Disk Wear Tracks in Steel System.

### 4.1.3 A-R-A + B-R'-B Type Compounds

The second new class of compounds tested consisted of two different difunctional molecules capable of condensation polymerization. These were dimethyl terephthalate and tert-butyl hydroquinone. The total wear for a 1 wt % molar ratio of these compounds in hexadecane are compared to the reference average in Figure 4.1.3.1.

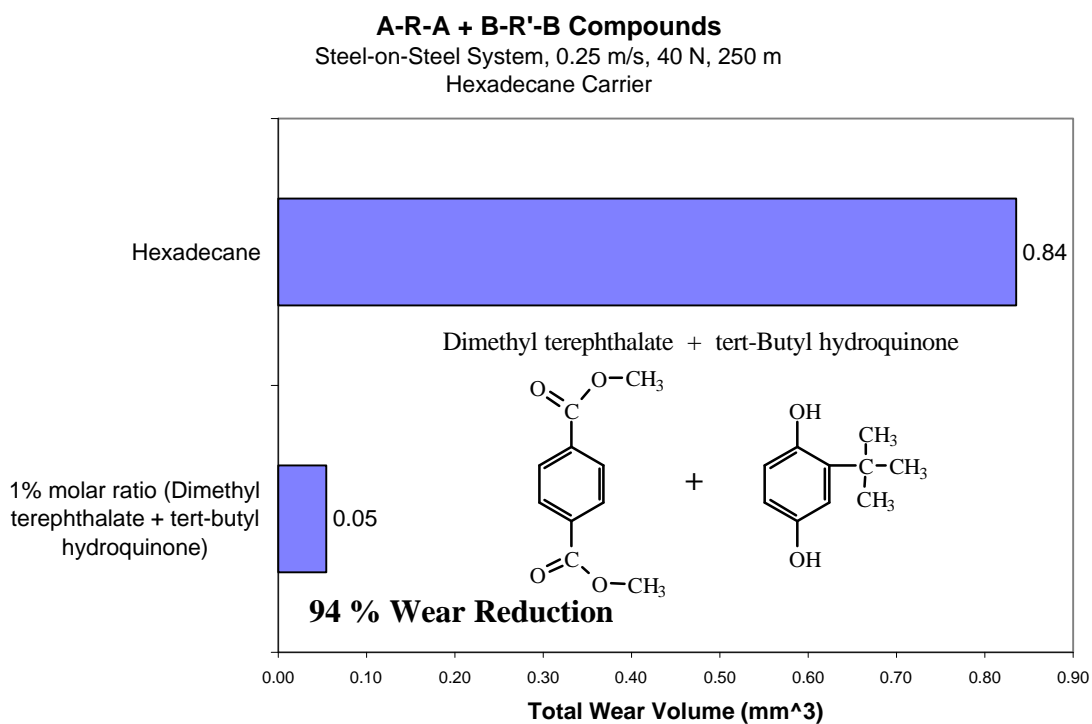


**Figure 4.1.3.1** Anti-wear Effect of A-R-A + B-R'-B Compounds Dimethyl Terephthalate and Tert-Butyl Hydroquinone in Steel System.

Photomicrographs in Figure 4.1.3.2 show attachment of wear debris observed on and near the disk wear track.

Dimethyl terephthalate + tert-Butyl hydroquinone

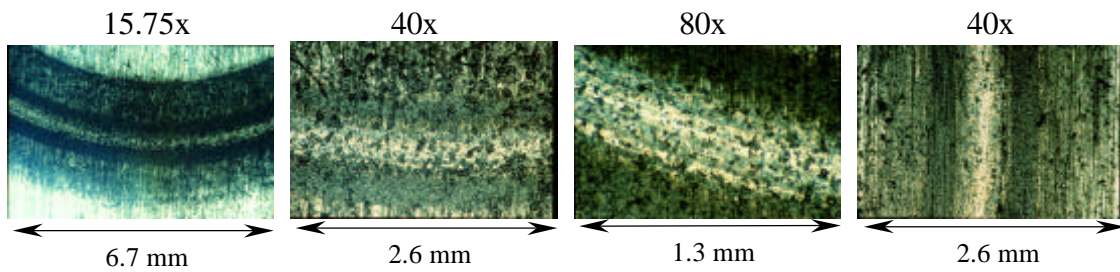
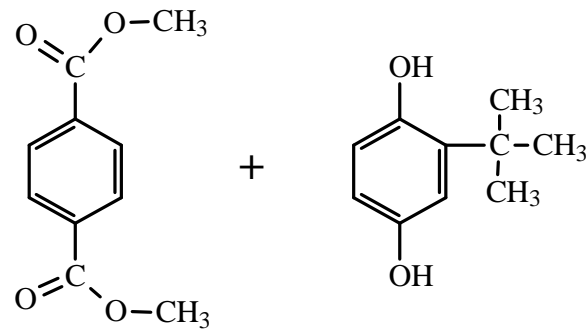


**Figure 4.1.3.2** Photomicrographs of Equimolar Mixture of Compounds Dimethyl Terephthalate and Tert-Butyl Hydroquinone Disk Wear Track in Steel System.

#### 4.1.4 Caprolactam

The last additive class tested in the Steel system was the heterocyclic amide caprolactam. Significant wear reduction was observed as demonstrated in Figure 4.1.4.1. Figure 4.1.4.2 shows some interesting crystallization near the wear track. The crystals formed slowly after test end and reflect the marginal solubility of the compound in hexadecane. This compound gave an interesting bronze colored wear pattern illustrated by the last four photomicrographs. After rinsing, the wear track remained shiny and unlike any of the reference test wear tracks.

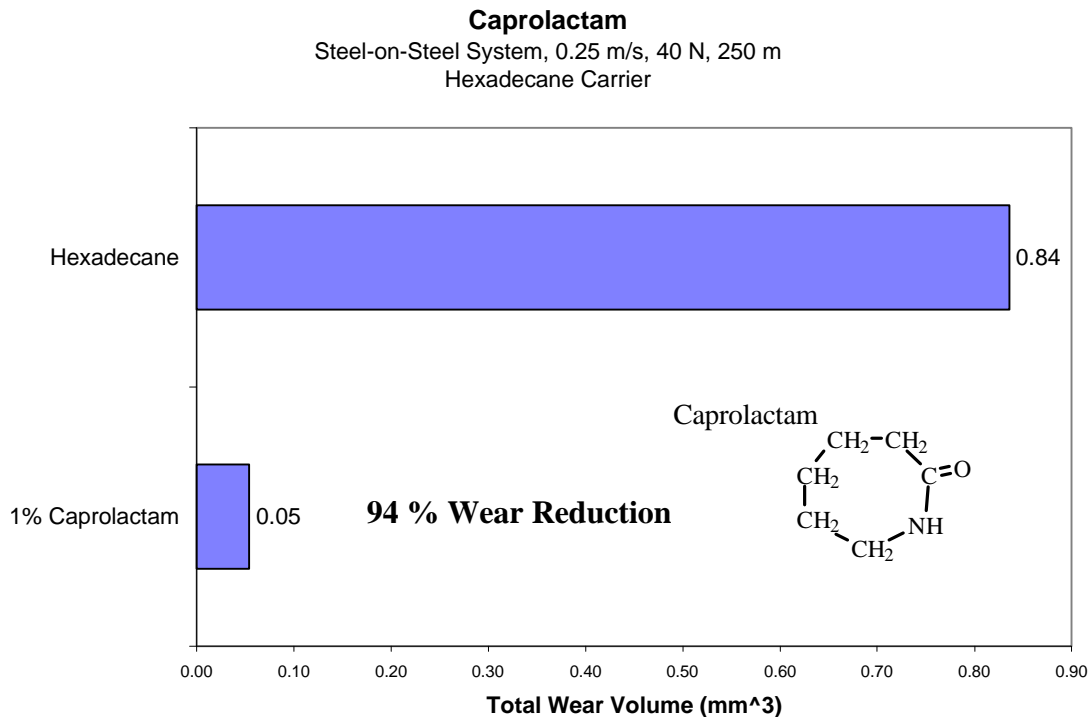


**Figure 4.1.4.1** Anti-wear Effect of the Heterocyclic Amide Caprolactam in Steel System.

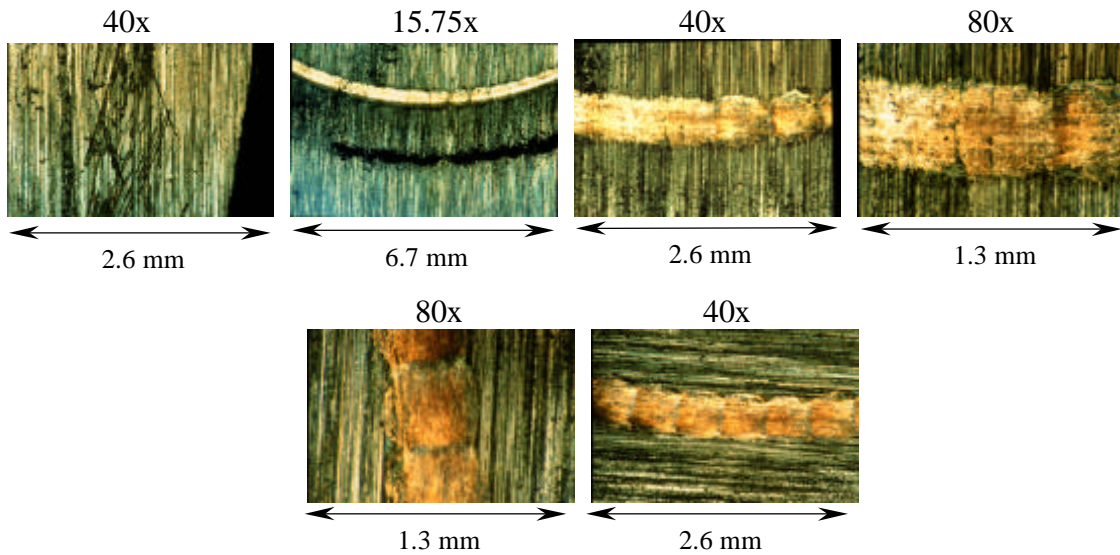
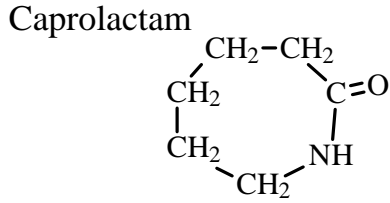


**Figure 4.1.4.2** Photomicrographs of Caprolactam Disk Wear Track in Steel System.

Based on the promising results from the Steel System, several candidates or similar configurations from each of these new classes of tribopolymerization additives were selected for further testing in the Alumina Systems. Wear results and photomicrographs are presented next for the higher wear rate of the two aluminas, the Alumina A System.